Journal of Photochemistry and Photobiology A: Chemistry 223 (2011) 172–181

Contents lists available at SciVerse ScienceDirect

Journal of Photochemistry and Photobiology A: Chemistry

journal homepage: www.elsevier.com/locate/jphotochem

Effects of the structure of entrapped substituted porphyrins on the textural characteristics of silica networks

M.A. García-Sánchez *, V. de la Luz, M.I. Coahuila-Hernández, F. Rojas-González, S.R. Tello-Solís, A. Campero

Department of Chemistry, Universidad Autónoma Metropolitana-Iztapalapa Av. San Rafael Atlixco 186, Col. Vicentina, P. O. Box 55-534, México D. F. 09340, México

ARTICLE INFO

Article history:
Received 4 February 2011
Received in revised form 30 July 2011
Accepted 18 August 2011
Available online 26 August 2011

Keywords:
Encapsulated photoactive porphyrins
Fluorescent silica
Cavity-size tailoring
Pore wall bonding
Functionalized alkoxides

ABSTRACT

The outstanding photoluminescent properties of porphyrin molecules in liquid solution were extended to solid media when these species were chemically trapped inside translucent, monolithic SiO_2 pore networks. The entrapment was made in situ through the sol–gel technique by adding to the relevant macrocycle solution a functionalized silicon alkoxide, water, HCl, and (if required) a chemical agent that inhibited the aggregation or degradation of the porphyrin compound. The success in attaining solid materials that encapsulate and immobilize individual porphyrin molecules was not only based on the identity but also on the selection of the appropriate molar concentrations of the above reactants. It was found that the cavity sizes in which porphyrin molecules were encapsulated depended on the structure of the macrocyclic species as well as on the type of alkoxide used to structuralize the silica network. In principle, the sizes of the cavities containing the porphyrin molecules could be modulated in four possible ways: (i) by the physical insertion of the macrocycle species in the pore network; (ii) by linking porphyrin molecules endowed with specific end groups of given lengths to the pore walls; (iii) by using functionalized silicon alkoxides that create linking chains extending from the pore walls toward the macrocycle species (possibility not treated here); (iv) by affording the porphyrin and silicon alkoxide molecules with suitable functional groups that established a long covalent linking between the macrocycle and the pore walls. In these ways, the average cavity width usually varied from 2.0 to 3. 6 nm but this interval could even be extended from 3.6 to 9.4 nm. The whole picture of porphyrin encapsulation in porous media involved: (i) the creation and modulation of assorted cavity sizes, (ii) the modification of the polarity of the pore surface by the attachment of functionalizing molecules, and (iii) the permanence of the luminescent properties of porphyrin molecules when these are covalently encapsulated inside silica substrates.

1. Introduction

Porphyrins play important roles in phenomena such as cell respiration, photosynthesis, and electron transfer [1] and involve important optical and electrical properties that allow a great number of applications in modern technology [2,3]. Species such as the free bases of porphyrins are photochemical pigments, which can be used as high-density information storage devices [4–7]. In photodynamic therapy (PDT) some fluorescent free bases of porphyrins can be selectively absorbed and subsequently released to kill cancerous cells through the generated oxygen singlet when the macrocycles are irradiated with red laser light (λ = 630–800 nm) [8–10]. It is well known that many porphyrins show red fluorescence [11] and also that optimal tissue penetration occurs when using light with a wavelength between 650 and 800 nm.

In order to exploit the important properties of porphyrins, it is in some cases necessary to trap or fix them within solid networks such as polymers [12]. Porphyrins cannot be inserted inside inorganic pore matrices by thermal diffusion because of their organic nature; besides, the impregnation method renders heterogeneous and lowly concentrated hybrid materials [13]. Nonetheless, during the last decades, little attention has been paid to the problem of efficiently trapping or fixing porphyrins inside inorganic pore networks and only a few methods have already been reported [14–21]. Still, the covalent bonding of these species to inorganic substrates has not been clearly assessed [22,23]. In particular, the free base of tetraphenylporphyrin, H_2TPP, involves a high nonlinear refraction coefficient [24]. This and some other important applications have conveyed considerable efforts with the purpose of efficiently insert macrocyclic molecules inside amorphous porous materials [12,15,17,25–28].

* Corresponding author. Tel.: +52 55 58044677; fax: +52 55 58044666.
E-mail address: mags@xanum.uam.mx (M.A. García-Sánchez).

1010-6030/$ – see front matter © 2011 Elsevier B.V. All rights reserved.
doi:10.1016/j.jphotochem.2011.08.015

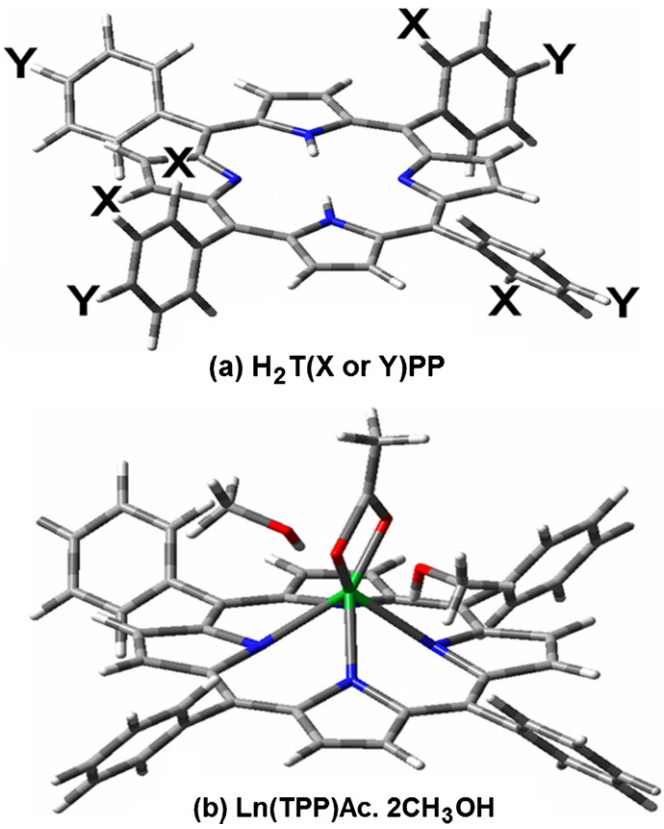

Fig. 1. Structures of: (a) *ortho* (*X*) or *para* (*Y*) substituted porphyrin free bases, $H_2T(X$ or $Y)PP$ (X or Y = –NH_2, –OH, –COOH, –SO_3H, etc.), and (b) lanthanide porphyrinic species, Ln(TPP)Ac.2S. (Ln = Lu, Yb, Tm, Er and Ho, and S = methanol, pyridine, etc.)

The sol–gel process allows the preparation of a great number of hybrid systems consisting of inorganic–organic [29–32] or biological molecules [33] trapped inside sinuous oxide networks resulting from the hydrolysis and polycondensation reactions of inorganic or organometallic precursors. The sol–gel route makes possible the creation of new and sophisticated nanocomposites, powders, thin films, monoliths, and ceramics through a soft chemistry or *chimie douce* [34,35] approach without the necessity of employing extreme thermal or chemical conditions. For optical applications, these systems are expected to be translucent substrates constituted of very small pores, preferably having no hydroxyl groups attached to the pore surface. For catalytic applications, it is essential to exert an adequate control of the pore size for permitting an efficient diffusion of reagents and products.

The aim of this research is to design photoactive translucent materials based on the encapsulation of porphyrins and related species, which are chemically trapped or physically enclosed within inorganic matrixes generated by the sol–gel technique. The present manuscript describes the trapping of *meso*-5, 10, 15, 20-tetraphenylporphyrins (TPP) substituted at the *ortho* (*X*) or *para* (*Y*) positions of the phenyls, $H_2T(X$ or $Y)PP$, with different groups, such as –NH_2, –OH, –COOH, –SO_3H, etc. (Fig. 1a) or their respective complexes (i.e. those endowed with different metals or substituent groups, Fig. 1b) inside the pores of a silica network generated from the hydrolysis and condensation reactions between *tetraethoxysilane* (TEOS) and water in the presence of HCl.

Furthermore, a description is made about a method of covalently fixing macrocyclic species inside the pores of silica networks through the combined use of TEOS and functionalized alkoxides (FA). The experimental findings demonstrate that, through the sol–gel process, a porous silica matrix can be generated around dissolved macrocyclic species while the pore size, pore shape, and texture are dependent on the structural characteristics of the trapped macrocyclic species. In other words, it is possible to control the textural parameters of the inorganic pore network obtained by the sol–gel method and the design of advanced materials can be achieved through the combined use of porphyrins and related macrocycles. The ultimate objective of this type of studies is to preserve, in the hybrid materials, the valuable properties that these macrocyclic species display in solution and to make profit of them in various fields such as optics, gas sensoring, catalysis, photocatalysis, and photomedicine.

2. Experimental

Lanthanide tetraphenylporphyrin acetates, Ln(TPP)Ac.2S (Fig. 1b) (Ln = Ho, Er, Tm, Yb, and Lu) were synthesized by the García-Sánchez method [19,36]. In turn, the *ortho* (*X*) and *para* (*Y*) substituted tetraphenylporphyrins, $H_2T(X$ or $Y)PP$ (X = –OH, –NH_2 or Y = –OH, –NH_2 and –COOH) (Fig. 1a), were synthesized by the Rothemun reaction [37] and the Adler method [38,39].

Macrocyclic species, such as porphyrins, could be physically trapped in ordinary translucent silica xerogels or inside particular organo-substituted silica matrices proceeding from the hydrolysis-condensation of TEOS under acidic (aqueous HCl) conditions (Fig. 2, Route (a)). Adequate molar combinations of TEOS and organo-substituted alkoxides (OSA), such as vinyl-triethoxysilane (VyTEOS) or ethyl-triethoxysilane (EtTEOS), were used to produce organo-substituted (i.e. surface-functionalized) matrices (Fig. 2, Route (b)). The previous materials were obtained from mixtures involving the following reactant molar ratios: [H_2O:TEOS + OSA and/or FA:HCl: Macrocyle or H_2P-F] = [$19.6{:}1{:}10^{-3}{:}10^{-3}{-}10^{-6}$], respectively, rendering a final total volume v_f [17–21]. A given quantity, on a percent volume basis (% v/v_f), of dimethylformamide (DMF), pyridine (py), methanol (MeOH) or combinations of these liquids was added to the reactant mixture to prevent aggregation, demetallation, and protonation of the macrocycle complexes. Similar systems, with the macrocycles covalently bonded to the pore walls (Fig. 2, Routes (c) and (d)), were prepared after combining TEOS with FA species such as; isopropyl-triethoxysilane (IPTES), aminopropyl-triethoxysilane (APTES) or N-(2-amino-ethylamine)-propyl-trimethoxysilane (NAEPTMOS), and monomers as 1,6-hexanodiamine (*Hexa*).

The formation of the precursory H_2P-F species and their union to the pore walls were confirmed and followed by FTIR spectroscopy. The mixtures were poured inside closed plastic cells, and the gelling process was monitored by UV–Vis spectroscopy. When the gel contraction step ended, samples were dried for three weeks at room temperature, afterward for three days at 70 °C and finally one day at 125 °C. The samples were characterized by FTIR, NIR, ^{29}Si-NMR (results not shown here), fluorescence spectroscopy as well as by powder X-ray diffraction, and N_2 sorption.

The UV–Vis–NIR characterization was carried out in a Cary–Varian 500E spectrophotometer from 200 to 800 nm (UV–Vis) and from 1000 nm to 2500 nm (100,000–4000 cm^{-1}) (NIR). The fluorescence studies of the solid samples were performed in a Perkin-Elmer LS 5 spectrofluorometer. The FTIR spectra were obtained from a Perkin-Elmer GX FTIR spectrometer. The N_2 adsorption–desorption experiments were measured in an Automatic Volumetric Quantachrome Autopore 1L-C instrument at 76 K (boiling point of N_2 at México City is 2250 m altitude). HRSEM images were obtained by means of a JEOL 7600F Instrument equipped with an Oxford Instruments INCA EDS detector.

Pore widths, inherent to the silica matrix containing macrocyclic species, were approximately calculated by the BJH method applied to the boundary adsorption curve of the N_2 isotherms

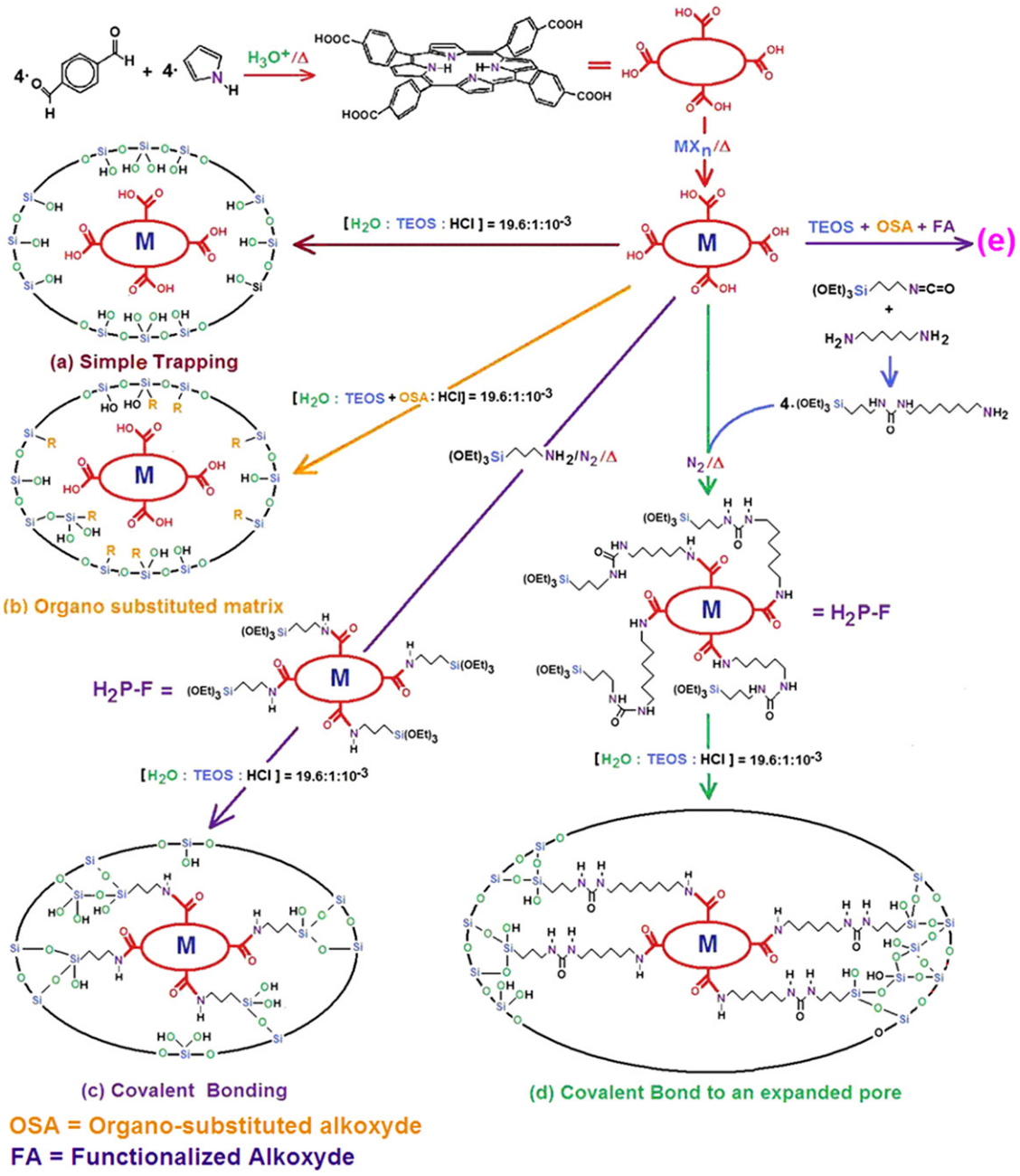

Fig. 2. Possible routes for the encapsulation of macrocyclic species inside SiO_2 xerogels: (a) physical entrapment in unfunctionalized silica, (b) entrapment in an organo-modified silica matrix, (c) covalent bonding of a functionalized macrocycle to the pore walls through functionalized alkoxydes, and (d) trapping inside expanded pores created by elongated bridges existing between the macrocyclic molecules and the pore walls. Route (e) is not pursued here.

[40]. It is known that the BJH approach underestimates pore sizes by at least 1.0 nm [41], when the void widths are smaller than 10.0 nm, although this determination becomes very approximate beyond this limiting width. Most times, as in the present case, the employment of desorption and adsorption data leads to two different BJH pore size distributions, thus revealing the existence of irreversible condensation and evaporation phenomena, which are usually linked to the presence of wide pore cavities interconnected by narrow throats throughout the network. In general, we expected to have such kind of pore structures in our SiO_2–porphyrin systems; nonetheless, the cavity sizes produced by the entrapment of macrocycles should better be calculated in the future from an elliptical (in view of the porphyrin molecule shape) pore model. Furthermore, a more realistic approach (Monte Carlo-Grand Canonical or Non-Local Density Functional Theory) could be employed for obtaining more precise pore-size distributions. In this work, we have employed, for the sake of simplicity, a cylindrical pore model.

3. Results

When a silica gel precursor, such as TEOS, reacts with water under acid or basic conditions, a solid network starts arising from the liquid mixture through the formation of a polysiloxane matrix (–Si–O–Si–), which can then endure the structural tensions. The pursuance of polycondensation reactions throughout the developing gel matrix causes the reinforcement, contraction, and

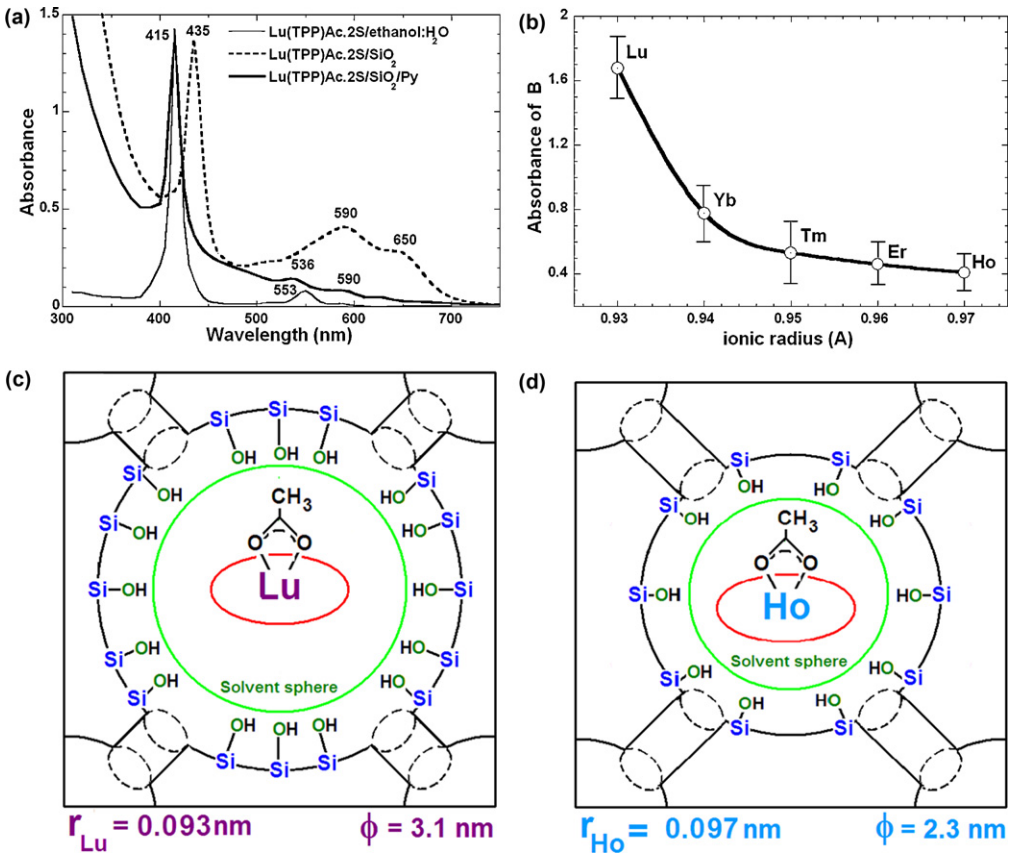

Fig. 3. (a) Ln(TPP)Ac.2S molecules can be trapped in stable form inside the pores of silica xerogels by using py as stabilizing agent. (b) The absorbance of the Soret bands in the UV–Vis spectra or these materials is a function of the ionic radius (r_{Ln}). The average pore diameter of the cavities formed around the trapped macrocyclic species depend on the identity of the lanthanide atom existing in these complexes (c and d).

displacement of remnant liquid from the pore entities. Additionally, the silica matrix can be further reinforced by thermal or chemical treatments in order to generate monolithic xerogels, powders, ceramics, thin films, and hybrid materials [42]. Translucent monoliths can be synthesized, on the one hand, under acid conditions and highly porous powders can be obtained, other option is using basic catalysis [43].

3.1. Simple physical trapping of porphyrins inside silica networks

As it was previously reported [19], simple physical trapping of the Ln(TPP)Ac.2S red fluorescent species (Fig. 2)(For interpretation of the references to color in this text, the reader is referred to the web version of the article.) in silica xerogels was possible by solubilizing these macrocyclic compounds in a 50:50% v/v_f mixture of ethanol and water and by the incorporation to the gelling mixture of a small quantity of py (0.7% v/v_f.). Since two py molecules can be coordinated to the lanthanide complex (substituting the original two solvent molecules), they can act as inhibiting agent against demetallation and protonation of the macrocycle; the later phenomena could have been caused by HCl addition [42,43]. When xerogels encapsulating diverse Ln(TPP)Ac.2S species (where Ln = Lu, Yb, Tm, Er and Ho) were prepared in the absence of py, their color changed from yellow to green and the UV–Vis spectra showed a red-shifted Soret band and a prominent Q_I band at around 650 nm (Fig. 3a).(For interpretation of the references to color in this text, the reader is referred to the web version of the article.) This last band was assigned to the presence of the H_4TPP^{2+} dicationic species, proceeding from the demetallation and protonation of the macrocyclic complexes [1,2,44–47].

In the UV–Vis spectra of Ln(TPP)Ac.2S molecules trapped in silica xerogels and prepared with a certain amount of py, there appeared the characteristics signals of tetraphenylporphyrin complexes, which were located at around 415 nm (Soret band) and 536 nm (Q_{II} band). In the UV–Vis spectra of these complexes, the Soret bands progressively became the most intense when going from Ho to Lu (Fig. 3b). This phenomenon could be originated by the contraction of the lanthanide atom, which caused that the number of water molecules around the lanthanide complexes increased as the ionic radius (r_{Ln}) decreased from Ho to Lu. Actually, the macrocycle molecule diminished its interaction with the hydroxyl groups of the silica network and the band intensity became higher than before. Furthermore, the pore size values obtained for these materials ranged from 3.1 nm for the Lu sample down to 2.3 nm for the Ho-doped material (Fig. 3c) [19].

These results, together with the NIR spectra, confirmed that the amount of water molecules that surrounded the Ln(TPP)Ac.2S complex, increased when r_{Ln} decreased. Also, the population of surface silanol groups (Si–OH), which remained around the solvated macrocyclic complexes, was proportional to the water volume. The absorbance of NIR bands associated with surface silanol groups appeared at around 2200 nm [19,36] and was proportional to r_{Ln} (Fig. 4).

The siloxane bonds (Si–O–Si) were more abundant when additional water molecules existed in the neighborhood of the macrocycle molecule and, as consequence, larger silica cavities were formed around it. The Si–OH group population was diminished by the formation of more siloxane bonds when samples were treated at 325 °C. All these observations pointed out to the fact that the physicochemical characteristics of the gel matrix depended on the nature of the lanthanoid complex that was trapped inside. In

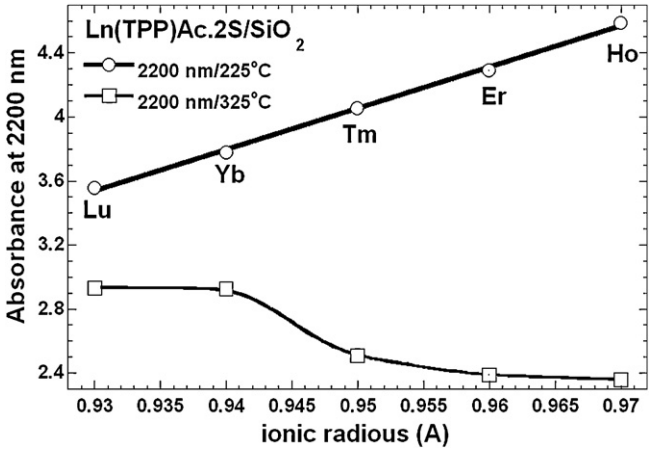

Fig. 4. (O) NIR absorbances of Si–OH surface groups, located at around 2200 nm and existing in the silica xerogels with the lanthanide complexes and treated at 225 °C, are proportional to the r_{Ln}. (□) However, this Si–OH population diminishes when the xerogel samples are annealed at 325 °C.

all these experiments, the red fluorescence of Ln(TPP)Ac.2S complexes, disappeared and only the blue fluorescence of the silica matrix prevailed [36].

After the formation of transparent and monolithic xerogels, the resultant solid volumes shrunk to only 10% of their original values. A set of UV–Vis spectra, taken at upper, middle, and bottom sections of these monolithic xerogels, just revealed the existence of a small Ln(TPP)Ac.2S concentration gradient along these three regions, as can be observed from the length extension of the Soret error bands depicted for each lanthanide complex shown in Fig. 3b. A HRSEM image of the Lu(TPP)Ac.2S sample (Fig. 5a) revealed a smooth surface while the corresponding EDS mapping analyses showed a uniform distribution of both carbon and nitrogen (Fig. 5b and c), which only can be due to the rather homogeneous distribution of the porphyrinic complexes throughout the xerogel network.

The insertion of the Ln(TPP)Ac.2S species in SiO_2 networks was possible in view of its solubility in water and ethanol; however, it should be noted that, in general, porphyrins are insoluble in polar solvents. Groups such as *–F*, *–NO_2*, *–NH_2*, *–OH*, *–SO_3H*, *–COOH*, and *pyridinium* when placed at the periphery of porphyrins made them, or their complexes, more soluble in polar solvents. To evaluate the effect of the nature and position of the substituents on: (i) the entrapment success, (ii) the final properties of the hybrid materials, and (iii) the attainment of optimal fluorescence, the methodology herein developed was extended to encapsulate, in stable form tetraphenylporphyrins that contained electron-attracting substituents, such as *–NH_2* (basic), or *–OH* (acid) groups in the *ortho-* or *para-* positions of the phenyls, H_2T(*X* or *Y*)PP or the respective metal complexes [17,18,21–23].

Initially, in order to design the method to trapping of functionalized (substituted) porphyrins in silica xerogels, the CoT(*X* or *Y*)PP (*X* = *o-OH* or *Y* = *p-OH* and *p-NH_2*) species was employed [22] as a probe molecule. It was found that for doing this, a high amount of DMF, py, or MeOH acting as demetallation inhibiting agents was necessary for nullifying the strong electro-attractive effect caused by the hydroxyl or amino groups located at *para* positions; however, a low amount of additives was enough to preserve stability when *ortho*-substituted porphyrins were employed. As was mentioned above, DMF, py and MeOH could be coordinated with the macrocyclic species thus inhibiting the approaching of other species to the central region of the complexes. The samples obtained were all optically translucent, rigid, xerogels in which there was clear evidence of a rather homogeneous distribution of the complexes. The BJH average pore sizes of these samples (obtained from N_2 sorption isotherms) varied in the range of 2.0–3.5 nm.

Similar experiments were carried out with porphyrin free bases [23] and the best results were obtained by including mixtures of

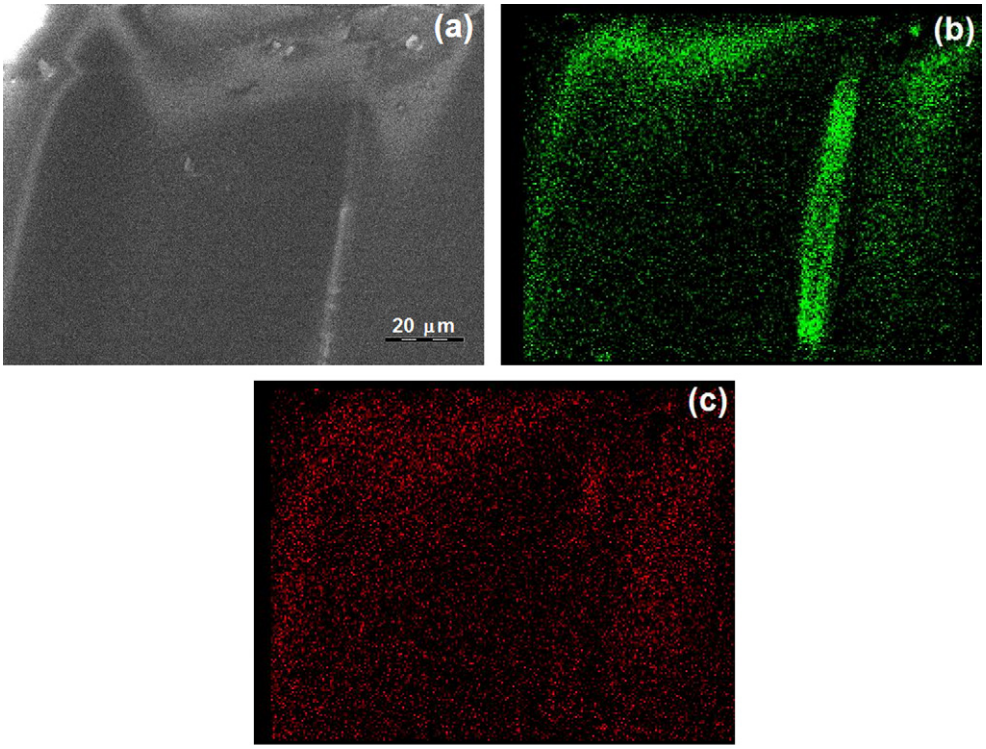

Fig. 5. (a) HRSEM image of the Lu(TPP)Ac.2S xerogel; EDS analyses reveal a rather uniform distribution of carbon (b) and nitrogen (c) throughout the structure. (For a better visualization of each element distribution the reader is referred to the to the web color version.)

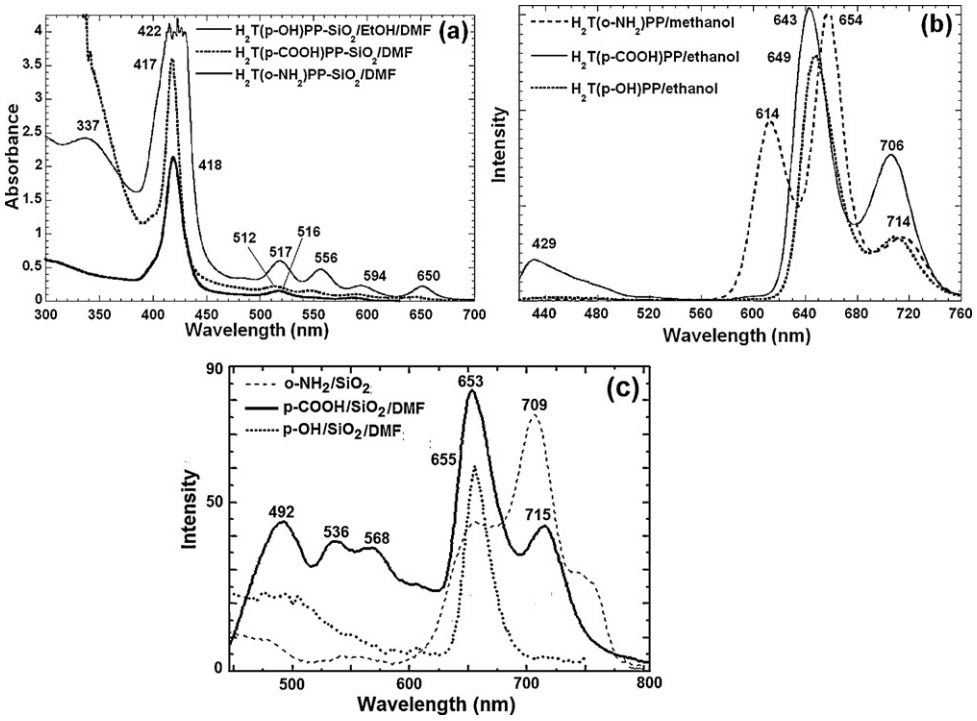

Fig. 6. When $H_2T(o\text{-}NH_2)PP$, $H_2T(p\text{-}OH)PP$, or $H_2T(p\text{-}COO)PP$ species are covalently bonded to the SiO_2 network, the UV–Vis spectra are similar to those displayed by these species in solution. A likewise situation is observed with respect to the fluorescence spectra of these species in solution (b) or when covalently bonded to the silica network (c).

DMF and py as inhibitors, yet the red fluorescence observed in the free porphyrin solutions, was only partially preserved in the gels prepared with the $H_2T(o\text{-}NH_2)PP$ species. This fluorescence inhibition could be caused by the interactions of the macrocycle with the Si–OH surface groups, in the tight pore environment and because of the different polarity existing inside the gel voids [23]. In these systems DMF, py and MeOH can only inhibit the protonation of porphyrin free bases but cannot prevent the interactions of the macrocycle with the Si–OH surface groups as the xerogel was being dried. In these amorphous translucent monolithic samples, the average pore width ranged from 2.2 to 3.5 nm. The largest cavity sizes were obtained when the *p*-substituted porphyrins were trapped and the shortest pore sizes corresponded to samples prepared with *o*-substituted porphyrins. These results reflected the effect of the position of porphyrin substituents on silica pore sizes and suggested that gel growth took place around the dissolved porphyrin molecules. Thus, the shape and size of the pores induced in SiO_2 matrices should be similar to the dimensions and shapes of solvated porphyrins.

In an attempt to eliminate the deleterious interactions between porphyrins and Si–OH surface groups, two methodologies were devised for inhibiting them: (i) to link porphyrin molecules to the silica surface by means of functionalized alkoxide (Fig. 2, Route c), or by (ii) extended bridges coming from the union of functionalized alkoxides and monomers (Fig. 2, Route d). Besides, (iii) an another option is to substitute the Si–OH surface groups by *alkyl* or *aryl* groups, thus changing the polarity inside the pores of the gel by using combinations of TEOS with organo-substituted alkoxides OSA (Fig. 2, Route b). Nevertheless, this last option was not pursued here, but it is still under study.

3.2. Covalent bonding of porphyrins to the pore walls of silica networks

The insertion technique methodology developed here was extended to the encapsulation of diverse porphyrinic species, such as free bases of substituted tetraphenylporphyrins, $H_2T(X$ or $Y)PP$, which depicted important luminescent properties. As it was previously said, some fluorescent porphyrin free bases could be selectively absorbed on living tissue and used to kill cancerous cells through the oxygen singlet generated when the macrocyclic molecules were irradiated with red laser light [8–10]; and since many porphyrin free bases fluoresce in the optimal tissue penetration range [11].

The presence of adequate substituent groups anchored on the periphery of the $H_2T(X$ or $Y)PP$ species made possible the covalent bonding of this molecule to the pore walls of the silica matrix through the bridging action of FA species, such as APTES, IPTES, or NAEPTMOS. By means of these connecting links, it was possible to establish covalent unions between the trapped macrocyclic species and the silica pore walls and then to take advantage of the enhanced properties of these hybrid systems. In particular, covalent unions bond porphyrins in stable and neutral forms to the silica matrix while preserving their inherent fluorescence. Thus, when porphyrins were covalently bonded to the silica network, the fluorescence remained and the respective spectra were very similar to those displayed by these molecules in solution. The latter occurred inasmuch as the covalent union reduced the interaction between the macrocycle and the matrix (i.e. the macrocycle was free) as well as the possibility of a non-radiating decay [48–50].

Additionally, the free $H_2T(X$ or $Y)PP$ (where $X = o\text{-}NH_2$ or $Y = p\text{-}COOH$, $p\text{-}OH$) were successfully bonded to the silica matrix by means of IPTES or APTES. The formation of a covalent union between the substituent groups of porphyrins and the functional groups of the above alkoxides rendered H_2P-F precursors (Routes (c) and (d) in Fig. 2). The existence of this covalent union was previously proved by monitoring the pertinent reactions through FTIR spectroscopy [48–50]. In a second step, the H_2P-F species was bonded to the polysiloxane chains generated from the hydrolysis and polycondensation of TEOS.

The UV–Vis spectra of the free porphyrin bases showed a prominent Soret band at around 420 nm and four bands of lowering absorbance, in the range extending from 500 to 700 nm, and labeled

as $Q_{IV} - Q_I$ [1,2]. When the free porphyrin is covalently bonded to the silica matrix, the respective UV–Vis spectra of all related xerogels showed that macrocycles existed, in stable form (i.e. disaggregated) in the interior of the pores (Fig. 6a). In case that the $H_4T(X$ or $Y)PP^{2+}$ dicationic species existed chemically bonded to the pore walls, the original neutral species could be restored through a series of deprotonation washings with either weak alkaline solutions or ethanol. This fact demonstrated that, these latter hybrid solids consisted of macrocycle molecules chemically immobilized inside the interconnected pore network, and remain in the structure during and after the completion of the washing procedure. By the same reason, the evaporation of fluids during the xerogel shrinkage step generated none macrocycle concentration gradient.

The fluorescence spectra (λ_{exc} = 370 nm) corresponding to the $H_2T(p\text{-}COOH)PP$, $H_2T(o\text{-}NH_2)PP$, and $H_2T(p\text{-}COOH)PP$ species in solution showed a prominent emission bands at 643, 649, and 654 nm, respectively (Fig. 6b). In the present work, the red fluorescence remained even after the porphyrin species were covalently bonded to the pore walls. The most intense florescence was obtained with the $H_2T(o\text{-}NH_2)PP$ compound, which spectrum showed a maximum at 709 nm; nonetheless, the spectra of the $H_2T(p\text{-}OH)PP$, $H_2T(p\text{-}COOH)PP$ xerogels (Fig. 6c), were similar to those displayed by the same molecules in solution (Fig. 6b). In these spectra the decrement in intensity of the 649 nm and 614 nm bands, displayed by the $H_2T(o\text{-}NH_2)PP$ and $H_2T(p\text{-}OH)PP$ species in solution (Fig. 6b), could be attributed to the different chemical environment existing in the interior of the silica pores or to the interactions with Si–OH surface groups.

A comparative fluorescence measurement between the $H_2T(X$ or $Y)PP$ species physically grafted or covalently bound to the silica xerogels confirmed that, in the first case, the relatively high interactions of the macrocycles with the –SiOH surface groups inhibited fluorescence, while in the second case fluorescence was preserved.

N_2 sorption at 76 K on the hybrid silica substrates produced Type IV or Type isotherms, which are typical of porous structures and the average pore widths ranged from 1.6–1.8 to 4.0 nm with specific surface areas varying from 459 to 632 m^2/g. In these samples, as well as in those in which free porphyrins could be simply trapped, the smallest pore sizes corresponded, again, to xerogels prepared with the *o*-amine substituted porphyrins and the largest pore sizes to porphyrins endowed with substituent groups located in the *p*-positions, i.e., on the same molecular plane of the macrocycle (Fig. 7a and b).

On comparing the pore sizes of the samples prepared with the $H_2T(o\text{-}NH_2)PP$ species either physically grafted or covalently bonded to the pore surface, we could confirm that, in the first case, a pore diameter of 2.0 nm was obtained since the matrix was formed at the periphery of the porphyrin solvation sphere. Keeping in mind that porphyrins have sizes of about 1.7 nm [1,2,44,46,47], it is possible to suppose that the above pore sizes are mainly due to the interactions existing between the Si–OH groups of the polysiloxane chains and the polar solvent molecules that are surrounding them and which interact, besides, with the $-NH_2$ groups that are located at the top and bottom of the porphyrin plane.

In other words, the dimensions of the macrocycle defined the size of the cavity in which it was trapped. Nonetheless, in the case of porphyrins covalently bonded to the silica matrix, fluorescence was preserved and the pore size of 1.6 nm was ruled by the length of the $-NH-CO-NH-(CH_2)_3-$ bridges formed when $-NH_2$ porphyrinic groups react with the isocyanate groups of IPTES. By the same reason, larger pore sizes were obtained when *p*-substituted porphyrins (with $-NH_2$, –OH, and –COOH groups) were bound to the silica matrix through functionalized alkoxides (Fig. 7a). These larger sizes could be due to the low polarity and length of the bridges formed at the periphery of the macrocyclic species when the substituent groups were located on the porphyrin plane.

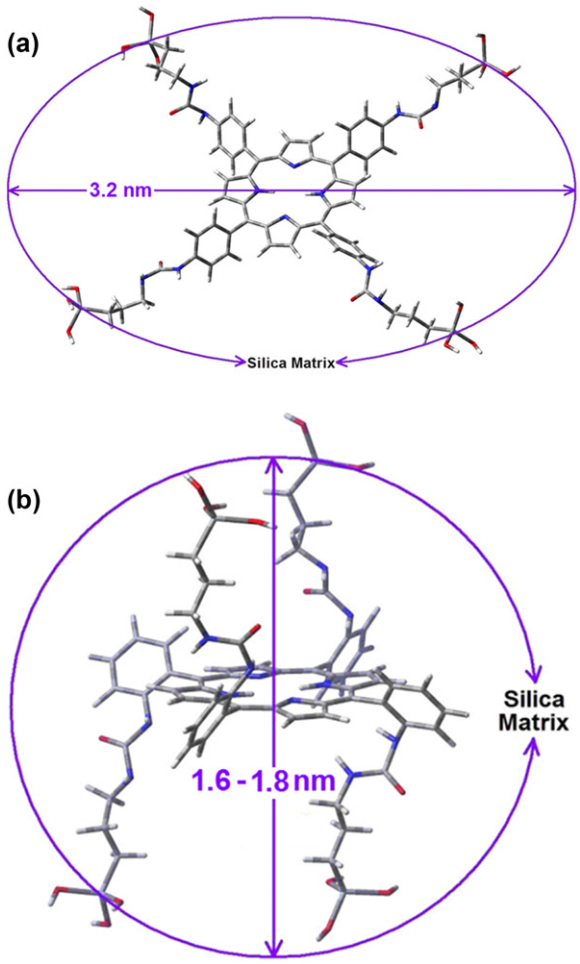

Fig. 7. The average pore width (Φ) values varied from 1.6 to 1.8 nm to 3.2 nm when (a) $H_2T(p\text{-}NH_2)PP$ and (b) $H_2To(p\text{-}NH_2)PP$ species are bonded to the pore walls of the silica matrix.

Actually, the cavity sizes were consequence of the ellipsoidal-like shape of the porphyrin molecule. As it was previously said, while the pore cavity is built around the porphyrin molecule, the pore size and shape depended upon the structure of the molecule that is being trapped or fixed to the gel matrix.

The HRSEM and EDS analyses of the latter samples (data not shown) revealed, once again, that the inserted macrocycles were likely to be homogeneously distributed throughout the glassy silica network, while N_2 sorption unveiled pore sizes around the lowest mesopore limit (i.e. 2.0–4.0 nm). As it was previously advanced (Fig. 2, Route c), the silica matrix systems herein described consisted of interconnected pores in which the transport of fluids was feasible while the interactions toward the trapped macrocycle molecules were relatively weak if compared to their strong covalent bonding to the silica matrix.

The methodology employed for immobilizing free porphyrins, could be extended for the trapping of the respective metalloporphyrin complexes. For instance, the $CoT(p\text{-}COOH)PP$ complex could be bound to the silica matrix by using APTES and 2% v/v_f DMF [49,51]. The UV–Vis spectrum of the last sample showed a Soret band at 432 nm and a Q_{III} signal at 544 nm, thus meaning that the porphyrin species remained in stable form inside the silica pores (Fig. 8).

After treating the $CoT(p\text{-}COOH)PP$ sample at 125 °C, the BJH analysis of N_2 desorption data rendered an average pore diameter of 2.7 nm and a specific surface area of 248 m^2/g. These values became 2.4 nm and 436 m^2/g after thermal treatment at 225 °C and

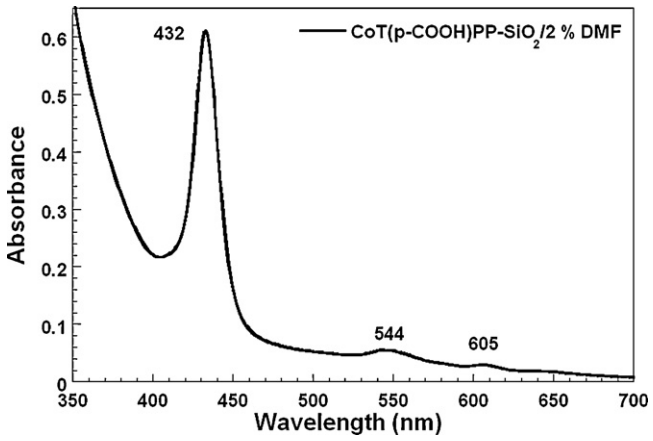

Fig. 8. UV–Vis spectrum of CoT(*p-COOH*)PP bonded to the silica network by using APTES molecules as bridges and 2.0% v/v_f of DMF as inhibiting agent.

2.0 nm and 343 m^2/g after annealing at 325 °C. The reduction in the average pore width (and consequent specific surface area increase) was caused by further water elimination and formation of siloxane bonds through condensation of neighboring silanol groups.

The formation of this siloxane unions reinforced the matrix structure and caused pore contraction and possibly the closing of some pore interconnections (Fig. 9). Also, the surface area increased by the elimination of most water and thermal decomposition of the macrocyclic complex. The latter facts showed that the final mean pore width was mostly determined by the size of the porphyrin complex, which length was around 1.7 nm [1,2,44].

With all previous experiences in mind, and on the basis of the synthesis and encapsulating methodologies developed above, our research was extended to the synthesis of new materials involving the coordination capacities of the encapsulated macrocyclic complexes [1,15–21]. Also, the modulation of the pore size could be accomplished by introducing of long bridges by the combined use of FA and other species and then the interactions porphyrin–silica could be adequately regulated.

3.3. Extended covalent bonding of porphyrins to silica networks

When 1,6-hexanodiamine reacted with IPTES an intermediary compound was formed, then the terminal amine of this intermediary complex reacted with the carboxyl groups of the H_2(*p-COOH*)PP species (Fig. 10) to yield an H_2P-F precursor (Fig. 2, Route d). Subsequently, this compound was reacted with TEOS and H_2O, in order to form polysiloxane chains around the porphyrin molecules, which were bonded to the silica network through a long hexanediamine-IPTES bridge (Fig. 10a). This two-step process was monitored by FTIR spectroscopy (data not shown). The xerogels obtained by this way were rigid, translucent monoliths

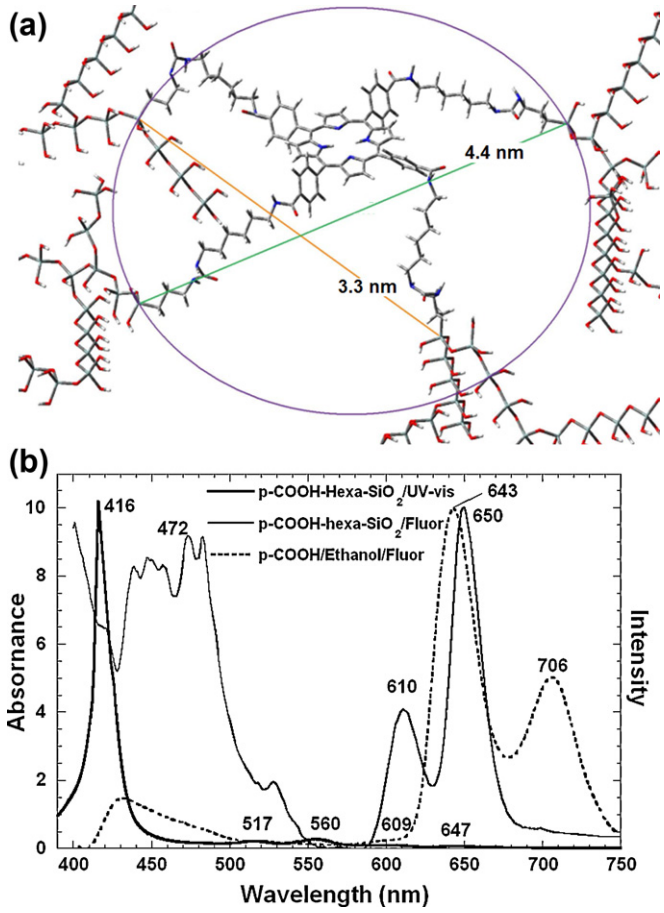

Fig. 10. (a) The H_2T(*p-COOH*) molecule could be bonded to the pore walls by creating pore cavities of average diameters ranging from 3.3 to 4.4 nm, through the reaction between hexanediamine (Hexa) and IPTES and subsequently with TEOS. (b) In these xerogels, the original UV–Vis and fluorescence spectra of the bonded macrocycle remained as that showed by the porphyrin solution.

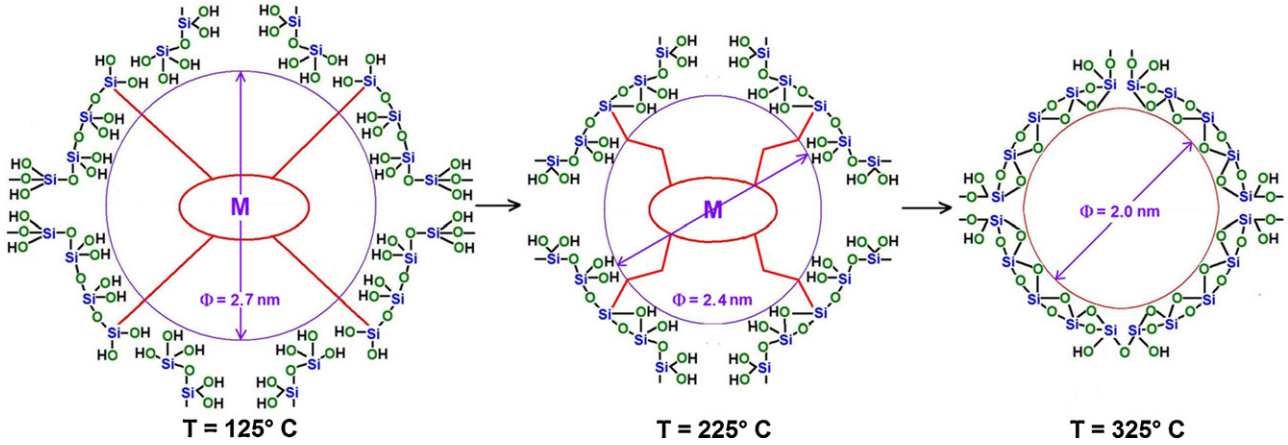

Fig. 9. The average pore width of samples containing species such as CoT(*p-COOH*)PP is a function of the size of the macrocyclic complexes as demostrated by N_2 sorption analysis after thermal tratments performed at 125, 225, and 325 °C.

which showed a red fluorescence similar to the observed in the corresponding porphyrin solutions (Fig. 10b). The maximum fluorescence band nm displayed by $H_2T(p\text{-}COOH)PP$ solution at 643 nm is red-shifted to 650 nm while the band at 706 nm disappeared when this species was bonded to the silica matrix through longer bridges. Additionally, a band at 610 nm was observed likewise a set of signals at around 472 nm, this last signal could be due to the blue emission caused by the silica network. These differences should be attributed to the different chemical environment and the interactions of the porphyrin with the Si–OH groups attached in the pore walls. The pore sizes ranged from 4.4 to 9.4 nm (Fig. 10a). The only explanation that could justify these relative large pore sizes was the formation of longer bridges with the pore walls consisting of two or more macrocyclic molecules joined to hexanediamine molecules. These results confirmed the possibility of enlarging and modulating the pore size of the xerogels through the use of macrocyclic species and the methodology herein reported.

By considering all the results herein presented, there now exists the possibility of controlling the size and shape of the pores embodying macrocyclic species encapsulated inside porous networks synthesized by the sol–gel technique. Also, it is possible to modify the internal physicochemical environment of the pores through the implantation of alkyl, aryl or organic functional groups on the pore walls by using suitable functional or organo-substituted alkoxides. The hybrid systems synthesized this way can be used in essential technological areas such as non-linear optics, medicine, gas sensoring, and photocatalysis.

4. Conclusions

The covalent bonding of porphyrin free bases or their respective complexes on the walls of porous networks produced translucent and monolithic silica xerogels. This was possible by mixing the adequate molar proportions of the following reactants: H_2O:TEOS:HCl:H_2P-FA. Additionally, diverse macrocycle complexes could be trapped in stable form, if additives such as DMF, pyridine, methanol or combinations of these were used for inhibiting porphyrin demetallation and protonation phenomena.

The interaction of the central regions of the porphyrin molecules with the silanol groups that were attached to the pore walls caused some important properties of these species (i.e. the fluorescence) to disappear. Nevertheless, these ill-effects could be thwarted when the macrocycle molecules were covalently trapped inside the pores of the silica network. Mechanistically, some deleterious phenomena over the macrocycles were inhibited by moving further away the porphyrin molecule from the surface silanol groups; this was made by establishing a large covalent union between the macrocycle and the silica matrix through the use of functionalized alkoxides, combined with other species (such as diamines or diacids). In this way the fluorescence displayed by the porphyrin free bases trapped inside the silica pores was similar to that shown by molecules in solution. Furthermore, the size and possibly the shape of the silica cavities that were formed around the solvated macrocyclic species depended of the nature and position of the substituent groups in the porphyrinic species.

Our recent results foresee the possibility of further controlling the textural properties of porous silica networks through the adequate selection and insertion of assorted macrocyclic species, such as substituted tetraphenylporphyrins. These hybrid substrates could become important in photocatalysis or catalysis, optics, medicine, and gas sensoring.

Acknowledgements

Thanks are due to the National Science and Technology Council (CONACYT) for the support provided through project No. 83659 "Estudio Fisicoquímico de la obtención y de las propiedades de los sólidos mesoporosos". Thanks are also due to the Ministry of Education (SEP) for the support provided to the Academic Bodies "Fisicoquímica de Superficies (CA 031)" and "Biofisicoquímica". Authors thank M. Sc. Patricia Castillo for her prompt and professional assessing with respect to the HRSEM and DSE analyses.

References

[1] K.M. Smith, Porphyrins and Metalloporphyrins, Academic Press, New York, 1978.
[2] D. Dolphin, The Porphyrins, Physical Chemistry, Part A and B, Academic Press, New York, 1979.
[3] Y. Liu, K. Shigehara, A. Yamada, Bull. Chem. Soc. Jpn. 65 (1992) 250.
[4] C. Fierro, A.B. Anderson, D.A. Scherson, J. Phys. Chem. 92 (1988) 6902.
[5] H. Inoue, T. Iwamoto, A. Makishima, M. Ikemoto, K. Horie, J. Opt. Soc. Am. B 9 (1992) 816.
[6] J. Friedrich, H. Wolfrum, D. Haarer, J. Chem. Phys. 77 (1982) 2309.
[7] C.C. Leznoff, A.B.P. Lever, in: C.C. Leznoff, A.B.P. Lever (Eds.), Phtalocyanines Properties and Applications, VCH Publishers, Inc., New York, USA, 1989.
[8] B. Ehrenberg, Z. Malik, Y. Nitzan, Photochem. Photobiol. 41 (1985) 429.
[9] G.G. Meng, B.R. James, K.A. Skov, M. Korbelik, Can. J. Chem. 71 (1994) 2447.
[10] T. Ben Amor, L. Bortolotto, G. Jori, Photochem. Photobiol. 71 (2000) 124.
[11] S. Salhi, M.C. Vernières, C. Bied-Charreton, J.A. Faure Revillon, New J. Chem. 18 (1994) 783.
[12] T.H. Wei, D.J. Hagan, M.J. Sence, E.W. Stryland, J.W. Perry, D.R. Coutler, Appl. Phys. B 54 (1992) 46.
[13] M. Hanack, M. Lang, Adv. Mater. 6 (1994) 819.
[14] H. Tanaka, J. Takahashi, J. Tsuchiya, Y. Kobayashi, Y. Kurokawa, J. Non-Cryst. Solids 109 (1989) 164.
[15] K. Kamitani, M. Uo, H. Inoue, A. Makishima, J. Sol-Gel Sci.Tech. 85 (1993) 85.
[16] X.J. Wang, L.M. Yates III, R.T. Knobbe, J. Lumin. 60–61 (1994) 469.
[17] M.A. García Sánchez, A. Campero, J. Sol-Gel Sci. Tech. 37 (1998) 651.
[18] M.A. García-Sánchez, A. Campero, Polyhedron 19 (2000) 2383.
[19] M.A. García Sánchez, A. Campero, J. Non-Cryst. Solids 296 (2001) 962.
[20] M.A. García Sánchez, A. Campero, J. Non-Cryst. Solids 333 (2004) 226.
[21] M.A. García-Sánchez, S.R. Tello-Solís, R. Sosa-Fonseca, A. Campero, J. Sol-Gel Sci. Tech. 37 (2006) 93.
[22] J.C. Biazzotto, H.C. Sacco, K.J. Ciuffi, C.R. Neri, A.G. Ferreira, Y. Iamamoto, et al., J. Non-Cryst. Solids 247 (1999) 134.
[23] J.C. Biazzotto, E.A. Vidoto, O.R. Nascimento, Y. Iamamoto, O.A. Serra, J. Non-Cryst. Solids 304 (2002) 191.
[24] M. Cervantes, M. Barboza, M. Inohue, J. Sov. Laser Res. 12 (1991) 447.
[25] A. Furusawa, K. Horie, I. Mita, Chem. Phys. Lett. 161 (1989) 227.
[26] W.P. Ambrose, W.E. Moerner, Chem. Phys. 144 (1990) 71.
[27] R. Locher, A. Renn, U.P. Wild, Chem. Phys. Lett. 138 (1987) 405.
[28] L. Bartoy, J.P. Lallier, P. Battioni, D. Mansuy, New J. Chem. 16 (1972) 71.
[29] D. Avnir, D. Levy, R. Reisfeld, J. Phys. Chem. 88 (1984) 5957.
[30] A. Makishima, T. Tani, J. Am. Ceram. Soc. 69 (1986) 4.
[31] J.C. Pouxviel, B. Dunn, J.I. Zink, J. Phys. Chem. 93 (1989) 2134.
[32] J. Fitremann, S. Doeuff, C. Sanchez, Ann. Chim. Fr. 15 (1990) 421.
[33] (a) N. Nassif, C. Roux, T. Coradin, M.N. Rager, O.M.M. Bouvet, J. Livage, J. Mater. Chem. 13 (2003) 203;
(b) Nat. Mater. 1 (2002) 42.
[34] (a) J. Livage, New J. Chem. 25 (2001) 1;
(b) J. Livage, M. Henry, C. Sanchez, Prog. Solid-State Chem. 18 (1988) 259.
[35] (a) C. Sanchez, L. Rozes, F. Ribot, C. Laberty-Robert, D. Grosso, C. Sassoye, et al., C.R. Chimie 13 (2010) 3;
(b) C. Sanchez, J.D.A.A. Soler-Illia Galo, F. Ribot, Grosso, C.R. Chimie 6 (2003) 113.
[36] M.A. García-Sánchez, Ph.D. Thesis, Universidad Autónoma Metropolitana-Iztapalapa, México, 2008.
[37] P. Rothemund, J. Am. Chem. Soc. 57 (1935) 2010, 61 (1939) 2912.
[38] A.D. Adler, F.R. Logo, F. Kampas, J. Kim, J. Inorg. Nucl. Chem. 32 (1970) 2443.
[39] A.D. Adler, F.R. Logo, J.D. Finarelli, J. Goldmacher, J. Assour, L. Korsakoff, J. Org. Chem. 32 (1976) 476.
[40] S.J. Gregg, K.S.W. Sing, Adsorption, Surface Area Porosity, Academic Press, London, 1982.
[41] M.L. Ojeda, J.M. Esparza, A. Campero, S. Cordero, I. Kornhauser, F. Rojas, Phys. Chem. Chem. Phys. 5 (2003) 1859.
[42] C.J. Brinker, G.W. Sherer, Sol–Gel Science, Academic Press, NY, USA, 1990.
[43] L.L. Hench, S.H. Wang, J.L. Nogues, in: Gunshor (Ed.), Multifunctional Materials, 878, SPIE, Bellingham, WA, USA, 1988, p. 76.
[44] M. Gouterman, in: D. Dolphin (Ed.), The Porphyrins, Physical Chemistry, Part A, Academic Press, New York, 1978.
[45] A. Stern, H. Wenderlein, Z. Physik. Chem. A 175 (1936) 405.
[46] A. Stone, E.B. Fleischer, J. Am. Chem. Soc. 90 (1968) 2735.
[47] G.D. Doroug, J.R. Miller, F.M. Huennekens, J. Am. Chem. Soc. 73 (1951) 4315.

[48] M.I. Coahuila-Hernández, M.A. García-Sánchez, A.M.E. Soto, A. Campero, J. Sol-Gel Sci. Tech. 37 (2006) 117.
[49] V. de la Luz, M.A. García-Sánchez, A. Campero, J. Non-Cryst. Solids 353 (2007) 2143.
[50] M.A. García-Sánchez, V. de la Luz, M.L. Estrada-Rico, M.M. Murillo-Martínez, M.I. Coahuila-Hernández, R. Sosa-Fonseca, et al., J. Non-Cryst. Solids 355 (2009) 120.
[51] M.I. Coahuila-Hernández, Ph.D. Thesis. UAM-Iztapalapa, México, 2011.